BULLETIN OF THE POLISH ACADEMY OF SCIENCES
TECHNICAL SCIENCES, Vol. 68, No. 5, 2020
DOI: 10.24425/bpasts.2020.134665

Surface based cohesive behavior implementation for the strength analysis of glued-in threaded rods in Glulam

T. GEČYS[1], G. ŠAUČIUVĖNAS[1], L. USTINOVICHIUS[2]*,
C. MIEDZIALOWSKI[3], and P. SULIK[4]

[1] Vilnius Gediminas Technical University, Faculty of Civil Engineering, Department of Steel and Composite Structures, Saulėtekio av. 11, LT-10223 Vilnius, Lithuania

[2] Vilnius Gediminas Technical University, Faculty of Civil Engineering, Department of Construction Management and Real Estate, Saulėtekio av. 11, LT-10223 Vilnius, Lithuania

[3] Bialystok University of Technology, Faculty of Civil and Environmental Engineering, ul. Wiejska 45a, 15-351 Bialystok, Poland

[4] The Building Research Institute, ul. Filtrowa 1, 00-611Warszawa, Poland

Abstract. The paper presents the analysis of strength and stiffness of metric threaded steel rods glued in glulam obtained by using two different gluing methods. The first method is used when the threaded steel rod is glued into a groove larger than the rod's diameter, while the second method is applied when the diameter of the groove is smaller than the diameter of the threaded steel rod. The steel rod is covered with glue before it is inserted into the smaller diameter groove. The first method investigates the 2-mm-thick glue-line, while the second method analyses the contact when the groove's diameter is 2 mm smaller than the outer diameter of the rod. Epoxy-type resin is used for both gluing methods. Different gluing methods present different interactions between the steel rod and glulam which result in different failure modes. The second method presents a plastic failure between the steel rod and glulam caused by the local compression and shear of glulam. The presented studies are made using metric threaded steel rods of diameters M12 and M16. In total, 20 specimens are experimentally tested in tension-to-tension tests performed according to EN 26891. The interaction between glulam and glued steel rods is also investigated using the 3D finite element modelling. The results obtained using the proposed 3D finite element model with different contact conditions between steel and glulam and the failure criterion for timber shear are well in line with the experimental findings.

Key words: glued-in rods, epoxy glue, finite element modelling, threaded steel rod.

1. Introduction

Glued-in steel rods present one of the most effective methods for connecting glulam elements when the contact between steel and glulam is ensured by glue. The stiff contact between the steel rod and glulam is achieved and relatively small deformations are measured at the failure moment, around 0.5–1.0 mm [1–3]. Due to high relative stiffness between the steel rod and glulam, glued joints may be used for beam-to-beam [4, 5] or column-to-foundation connections [6]. Glued-in steel rods are also used for strengthening of the old or newly built glulam structures [7]. Despite the wide range of applications of glued-in steel rods, now, no rules can be found in the current European timber design codes for determining the strength and stiffness parameters of glued-in steel rods. Currently, the updates are being prepared for the European timber design code Eurocode 5 [8]. The application of glued-in steel rods was limited to I and II service classes according to EC5, therefore, the investigations on the influence of moisture content [9] and fire safety [10, 11] were performed. The experimental investigations of glued-in steel rods using epoxy-type adhesives done at elevated temperatures have shown that the stiffness decreases while the bearing capacity remain the same [11].

Glued-in steel rods are usually glued into larger diameter grooves. The thickness of the glue-line varies in the range of 0.5–2 mm, depending on the glue type. The failure of this connection is usually brittle, as the bearing capacity is governed by timber shear. There are no evident plastic deformations between the timber and steel until the failure because the bond-line's thickness is relatively small. Lag-screw fasteners may be used as an alternative to the glued-in steel rods. These rods are usually screwed into the predrilled grooves with a diameter equal to, or close to, the inner diameter of the screw [12–14]. The thread height may be 1–3 mm, depending on the type of the lag-screw fastener. These screws are installed in the timber element without using any glue.

This paper also discusses two different methods of gluing-in threaded steel rods as follows: in the first method, the steel rod is glued into the groove with a larger diameter of 4 mm, and the second method is used when the diameter of the groove is 2 mm smaller and equals to the inner diameter of the threaded steel rod. The threaded steel rod has a longitudinal rectangular-shaped groove of 2×2 mm in the glued-in length. The lon-

*e-mail: leonas959@gmail.com

Manuscript submitted 2020-02-17, revised 2020-06-18, initially accepted for publication 2020-08-10, published in October 2020

gitudinal groove aims to distribute the glue layer equally during the screwing process when a part of the rod is covered with glue before it is inserted into the timber element. When the steel rods are glued into the smaller diameter grooves the interaction is very similar to the behavior of a lag-screw and timber. In this case, the failure of the connection occurs with no sudden load drop comparing with the first method. The epoxy-type glue is used for both gluing methods. The results of the experimental investigation presented below show their close agreement with the results obtained in finite element modelling in terms of bearing capacity and load-deformation behavior.

In practice, there are situations when glued-in steel rods are being used for strengthening or other specific situations not discussed in the design codes. For this reason, the understanding of actual behavior of glued-in rods is significantly important for structural timber engineers. There is big need of implementation of finite element analysis for the determination of strength and stiffness characteristics of glued-in rods in timber. Further in this article the implementation of the surface-based cohesive behavior is provided. The novelty of the article lies in the implementation of the quadratic stress criterion which was used to define the initiation of the damage in the predefined surface between glued-in steel rod and timber. The finite element analysis results are well in line with the experimental findings.

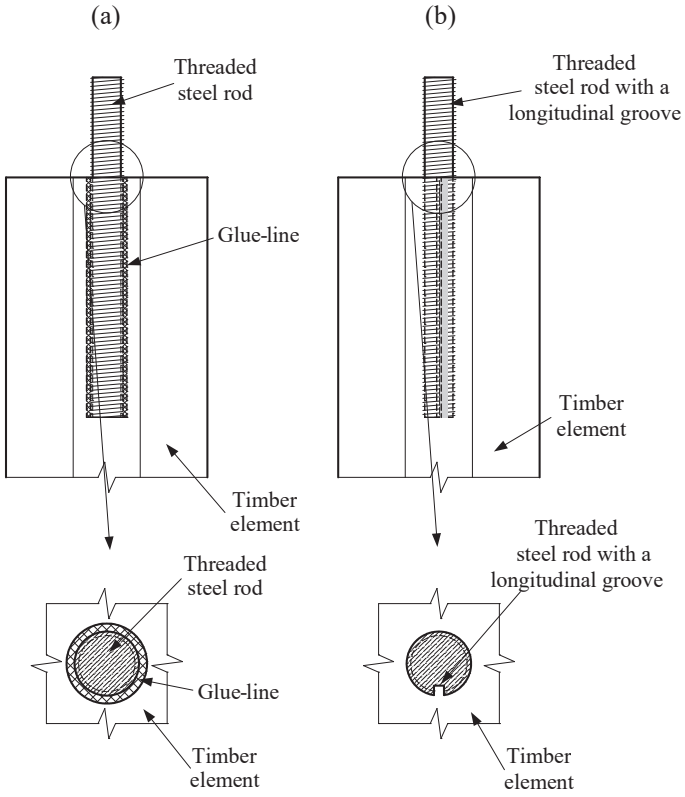

Fig. 1. Various methods for gluing-in the threaded steel rods

2. Gluing techniques and the test setup

2.1. Various gluing techniques. As shown in Fig. 1, two different gluing methods are discussed in the paper. In the first method, the predrilled groove is filled with glue before the insertion of the steel rod. The volume of the injected glue is equal to the volume of the groove minus the volume of the glued-in threaded rod. The threaded rod was slowly inserted into the glue-filled groove and twisted around the longitudinal axis to ensure equal distribution of the glue and to avoid air gaps. The discharged glue shows that the volume of glue is sufficient. The glue-line thickness was assumed to be equal to 2 mm, i.e. the groove's diameter is 4 mm larger than that of the nominal threaded steel rod. Using the glue-line of smaller thickness provides a possibility of obtaining the uneven distribution of the glue.

The second gluing method implies that the diameter of the groove is equal to the inner diameter of the threaded steel rod. The threaded steel rod has a longitudinal rectangular-shaped groove for better distribution of the glue during the process of its screwing into the timber element, as shown in Fig. 1b. The part of the rod glued in to the timber element is covered with glue before the screwing into the timber. While installing these types of connections the additional transverse breath-hole is drilled in the timber element to avoid the vacuum between the steel rod and the timber. In these investigations, the transverse breath-hole was not installed. The M12 and M16 metric threaded steel rods were used, and the diameters of the grooves were 10 and 14 mm, respectively. One third of the groove was filled with glue before the insertion of the threaded steel rod.

2.2. Materials. The experimental investigations were made using the homogenous glued laminated spruce timber of the strength class GL24h according to the standard EN 14080:2013 [15]. The cross section of the timber element was rectangular with the dimensions of 100×100 mm. The total length of the glued laminated timber elements was 340 and 420 mm for the steel rods of 12 and 16 mm in diameter, respectively. Various lengths of the timber elements were assumed to ensure the same distance of 100 mm between the glued-in steel rods during the tension-to-tension test. The anchorage length was assumed to be 10 times the diameter of the rods to avoid the uneven stress distribution along the rod length. M12 and M16 metric threaded steel rods of the 5.8 strength class were used in the experimental studies. For both gluing methods epoxy-type glue Hilti HIT-RE 500 was used. This type of glue may be used for gluing steel rods in concrete or timber. Threaded steel rods were glued into timber at the specialized glulam factory with the controlled ambient temperature and relative moisture content.

2.3. The set-up of the experimental test. The aim of these experimental studies is to determine the withdrawal capacity, stiffness and the failure mode of the glued-in threaded steel rod. Various gluing methods were investigated using the same geometrical parameter connections to see the differences in behavior. The experimental studies were performed at Vilnius Gediminas Technical University using the loading machine Tinius Olsen with the bearing capacity of 75 kN. The main exper-

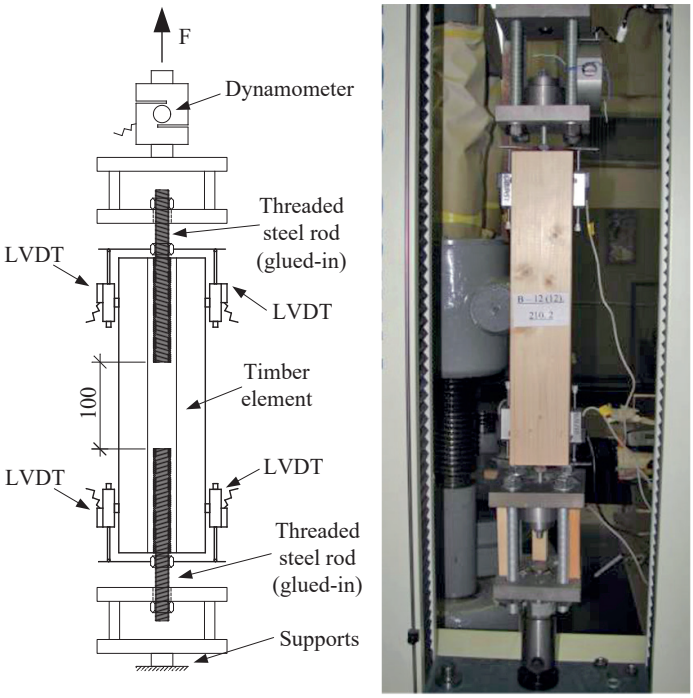

Fig. 2. The experimental setup of the tension-to-tension test

iment was the pull-to-pull tension test performed according to the standard EN 26891 [16], as shown in Fig. 2. According to the recommendations of the standard, the load was applied incrementally and included partial unloading and reloading. The experimental test was performed until the maximum load was achieved to determine the actual failure mode.

During the loading, the relative deformations were continuously measured with LVDTs attached to both ends of the specimen. The mean value of two opposed LVDTs was calculated for the data evaluation in terms of force-relative deformation relationships. The LVDT with the measurement length equal to 25 mm was taken. The applied load was displacement-controlled with the rate of 0.15 mm/min. The preliminary tests have shown that this value is appropriate for reaching the total testing time of 10–15 min. In total, 20 specimens were experimentally tested, as summarized in Table 1. Four different geometry test series were taken, with 5 specimens in each. The ratio of the anchorage length to the diameter was assumed to be 10 for all the specimens.

3. Finite element analysis

3.1. General data. The commercial finite element software Abaqus was used with the aim of simulating the behavior of the glued laminated timber element and the threaded steel rod [17, 18]. The 3D finite elements were used to define the interaction between the timber-glue line and the glue line-steel. The finite element model fully represents the geometry of the experimentally investigated specimen. The connection is symmetric in the planes x-y, x-z and y-z, therefore, to save the calculation time the finite element model is reduced to one quarter of the connection. The symmetry conditions are applied to the plane x-z which allows free deformation of the elements in the x and z directions, but free rotation is constrained about the y axis. The finite element model of the analyzed connection is shown in Fig. 3, where the fine mesh of all the elements is presented. Figure 3 presents both models of various gluing methods: a) the connection when the glue-line between the timber element and

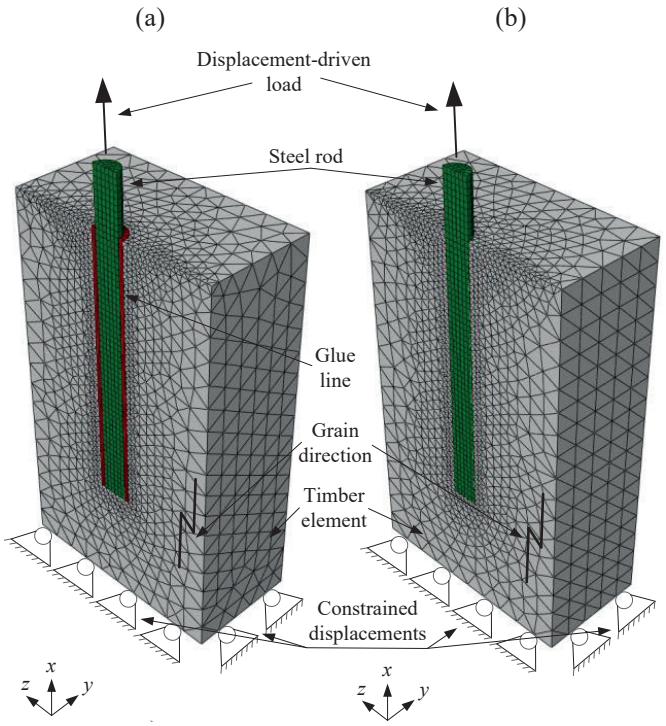

Fig. 3. Various finite element models of the connection: a) timber-filler--steel rod, b) timber-steel rod

Table 1
The geometrical data of the specimens

Name of specimen	Number of specimens	Cross section of timber (mm)	Steel rod diameter (mm)	Groove diameter (mm)	Anchorage length (mm)
S-12(16).120	5	100×100	12	16	120
S-12(10).120	5	100×100	12	10	120
S-16(20).160	5	100×100	16	20	160
S-16(14).160	5	100×100	16	14	160

the steel rod is modelled and b) the connection representing the direct contact between steel and glulam. The method when the steel rod is screwed into the smaller diameter groove with no glue-line is simulated (see Fig. 3b). The timber element is defined using a 4-noded tetrahedron element with the elastic-linear plastic material model. The material can be observed to undergo neither hardening nor softening effects. The steel rod was defined as a circular-shaped element with the diameter equal to the outer diameter of the rod. The steel rod was modelled using 8-noded linear brick elements with reduced integration and an isotropic elastic-plastic material model without any hardening and softening. The mentioned type of finite element was chosen after parametric analysis which showed the lowest calculation time without any negative effect on the calculation results comparing with the other type of finite elements. The glue-line was defined using the same type of the finite element as that used for the steel rod with the elastic material model. The finite elements of various sizes were used for the materials. The base dimension for timber was 10 mm with up to 2.5 mm refinement at the point of contact with the steel element or the glue line. The timber element mesh refinement was made in contact with the glue-line (Fig. 3a) and the steel rod (Fig. 3b). The size of the finite element of the steel rod was 2.5 mm and for the glue-line it was 1 mm to have at least two elements through the thickness of the layer. The displacements and rotations of all the nodes were fixed on the bottom, i.e. the y-z plane. The applied load was displacement-driven in the x direction set to the free end of the steel rod, up to 2 mm.

3.2. The material models, contacts and boundary conditions. The timber material is described as orthotropic material with two perpendiculars which are longitudinal in the x and transverse in the y and z directions. The physical and mechanical properties of timber were determined based on the density tests and the data taken from the previous investigations on the same strength class, as well as from the same glulam producer [19, 20].

For evaluating the nonlinear behavior of timber, a combination of two failure criteria was used. The Hill potential function was applied to capture the yielding under the compression along and perpendicular to the grain. The Hill criterion, which is an extended form of the von Mises criterion, reads as [21]:

$$f(\sigma) = \\ = \sqrt{\begin{array}{l} F(\sigma_{RR}-\sigma_{TT})^2 + G(\sigma_{TT}-\sigma_{LL})^2 + \\ H(\sigma_{LL}-\sigma_{RR})^2 + 2L\sigma_{RT}^2 + 2M\sigma_{TL}^2 + 2N\sigma_{LR}^2 \end{array}} \quad (1)$$

where:

$$F = \frac{(\sigma^0)^2}{2}\left(\frac{1}{\bar{\sigma}_{TT}^2} + \frac{1}{\bar{\sigma}_{LL}^2} + \frac{1}{\bar{\sigma}_{RR}^2}\right)$$

$$G = \frac{(\sigma^0)^2}{2}\left(\frac{1}{\bar{\sigma}_{TT}^2} + \frac{1}{\bar{\sigma}_{LL}^2} + \frac{1}{\bar{\sigma}_{RR}^2}\right)$$

$$H = \frac{(\sigma^0)^2}{2}\left(\frac{1}{\bar{\sigma}_{LL}^2} + \frac{1}{\bar{\sigma}_{RR}^2} + \frac{1}{\bar{\sigma}_{TT}^2}\right)$$

$$L = \frac{3}{2}\left(\frac{\tau^0}{\bar{\sigma}_{RT}}\right)^2$$

$$M = \frac{3}{2}\left(\frac{\tau^0}{\bar{\sigma}_{LT}}\right)^2$$

$$N = \frac{3}{2}\left(\frac{\tau^0}{\bar{\sigma}_{LR}}\right)^2$$

where $\bar{\sigma}_{ij}$ are the yield stresses, σ_{ij} are acting stress components, σ^0 is the reference yield stress and $\tau^0 = \sigma^0/\sqrt{3}$ [21]. The Hill criterion does not consider the difference in tensile and compressive strengths as well as the different failure modes, both along and perpendicular to the grain.

The second failure criterion was the surface-based cohesive behavior used to represent the failure upon the tension perpendicular to the grain and shear. The physical and mechanical properties of timber and the yield strengths which were used in the finite element analysis are summarized in Table 2. The more detailed application of the Hill potential function was described in the authors' previous papers [17]. The material of the threaded steel rod is characterized as the elastic perfectly plastic isotropic material with the modulus of elasticity and Poisson's ratio presented in Table 2. The glue-line material is assumed to be isotropic elastic, as listed in Table 2.

To evaluate the actual interaction between timber and steel, various contact types between the interacting materials were applied as follows: timber-to-glue, glue-to-steel and steel-to-timber. The contact between separate materials is defined by applying the surface contact properties. The contact between the threaded steel rod and the glue-line assumes perfect contact between the surfaces without relative motion and separation or friction. According to this assumption, the failure on the surface between the glue-line and the steel rod is not possible. Thus, no failure criterion is applied to this plane. The interaction between timber-to-glue (Fig. 3a) and timber-to-steel (Fig. 3b) is defined by applying the surface-based cohesive behavior. The cohesive contact properties were applied to this surface with the properties listed in Table 2. A more detailed explanation of the surface-based cohesive failure criterion implementation is provided in the previous publication of the authors [19]. There are three possible fracture modes in the predefined timber-to-glue and timber-to-steel surfaces. The failure expected to occur in the timber element is caused by the tensile stresses perpendicular to the grain (mode 1), shear stresses parallel to the grain (mode 2) and shear stresses acting out-of-plane of the grain direction (mode 3). The fracture may occur in each of these modes separately, as well as in the combination of these modes. A quadratic stress criterion was used to define the initiation of the damage as follows:

Table 2
The material properties used in finite element analysis

Elastic material properties of timber								
E_L [N/mm²]	E_R [N/mm²]	E_T [N/mm²]	ν_{LR} [-]	ν_{LT} [-]	ν_{RT} [-]	G_{LR} [N/mm²]	G_{LT} [N/mm²]	G_{RT} [N/mm²]
11 587	510	510	0.00894	0.00894	0.538	315.7	315.7	161.1

Plastic material properties of timber					
f_{LL} [N/mm²]	f_{RR} [N/mm²]	f_{TT} [N/mm²]	f_{LR} [N/mm²]	f_{LT} [N/mm²]	f_{RT} [N/mm²]
44.2	5.0	5.0	5.0	5.0	3.3

Cohesive failure properties of timber			
Model name	$f_{t,90}$ [N/mm²]	f_v [N/mm²]	$f_{v,90}$ [N/mm²]
S-12(16).120	4.86	7.29	4.86
S-12(16).120 (actual area)	3.54	5.30	3.54
S-12(10).120	3.05	4.57	3.05
S-16(20).160	4.14	6.21	4.14
S-16(20).160 (actual area)	3.18	4.78	3.18
S-16(14).160	2.28	3.43	2.28

Steel bolts		
E [N/mm²]	ν	f_y [N/mm²]
210 000	0.3	400

Glue-line		
E [N/mm²]	ν	f_y [N/mm²]
2 600	0.2	–

$$\left(\frac{\sigma_{t,90}}{f_{t,90}}\right)^2 + \left(\frac{\tau_v}{f_v}\right)^2 + \left(\frac{\tau_{v,90}}{f_{v,90}}\right)^2 = 1, \qquad (2)$$

where $\sigma_{t,90}$ is the tensile stress perpendicular to the grain, τ_v is the shear stress in the parallel direction to the timber grain, $\tau_{v,90}$ is the rolling shear stress and $f_{t,90}$, f_v, $f_{v,90}$ are the respective strengths of the timber element. The timber shear strength parallel to the grain is defined from the results of the experimental study by dividing the achieved maximum force F_{max} by the shear area. According to EC5 or any other methodology, the shear strength strongly depends on the diameter of the glued-in rod and the anchorage length. Therefore, the shear strength is separately determined for each model with the M12 and M16 rods. The failure of the surface with the applied cohesive properties occurs when the applied criterion according to Eq. (1) reaches the value of 1.0 in the whole surface area. The bearing capacity of the FE modelling is determined by summing up all support reactions from each node in the x direction.

Displacements in all directions are constrained of the bottom horizontal surface of the finite element model, as it is shown in Fig. 3.

4. The results of the experimental and numerical simulation

4.1. The experimental results. Various gluing methods present different behavior in terms of the relation of the failure mode to the load-relative displacement [22, 23]. The connection with the steel rod glued in the groove with a larger diameter shows brittle failure caused by the timber shear parallel to the grain, as shown in Fig. 4a. Depending on the annual growth rings and branches, the split off timber elements vary from the regular circular shape to the split off shear block. There could not be observed any plastic deformations right up to the point where the maximum load was reached. In the cases when steel rods are screwed with glue in the smaller diameter grooves the failure mode differs, showing ductile behavior at the time of failure [24].

The failure mode is the timber's local shear on the surface between the outer rod diameter and the timber, as shown in Fig. 4b.

The experimental withdrawal capacities F_{EXP} are summarized in Table 3. This shows relatively large differences between the bearing capacities when different gluing methods

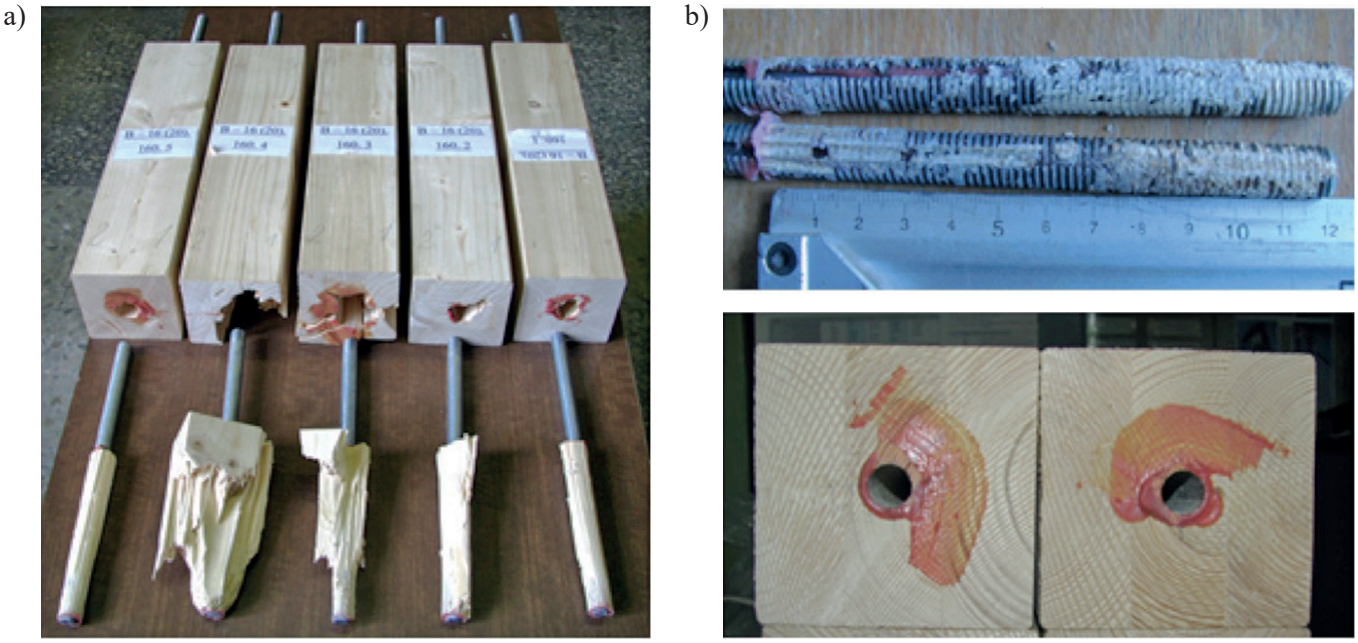

Fig. 4. The experimental failure modes characteristic of different bonding techniques: a) a steel rod is glued into a larger groove; b) a steel rod is glued into a smaller diameter groove

Table 3
The experimental and finite element modelling results

Name of specimen	F_{EXP} [kN] SD [%]	F_{FEM} [kN]	Ratio F_{EXP}/F_{FEM}	Experimental failure mode
S-12(16).120	43.96 2.6	32.68 34.00 (actual shear area)	1.35 1.29	Brittle/timber shear
S-12(10).120	17.21 28.1	16.22 –	1.06 –	Ductile/timber shear
S-16(20).160	62.39 9.8	47.39 49.04 (actual shear area)	1.32 1.27	Brittle/timber shear
S-16(14).160	27.53 22.7	23.39 –	1.18 –	Ductile/timber shear

are used. The differences for these methods are in the range of 2.26–2.55 times. The first gluing method (S-12(16).120 and S-16(20).160) shows more reliable results with the standard deviation of 2.6–9.8 %.

One of the parameters determining the withdrawal capacity of the glued-in steel rod is the diameter of the rod. The average curves of the shear stress-relative deformation for the different series of specimens are presented in Fig. 5. For specimens with the 2-mm-thick glue-line the shear stress at the failure moment is 7.29 and 6.21 N/mm^2 for M12 and M16 rods, respectively. For specimens with the 0-mm-thick glue-line the shear stress at the failure moment is approximately 1.7 times smaller than that for the specimens with the 2-mm-thick glue-line. This difference can be accounted for by the fact that

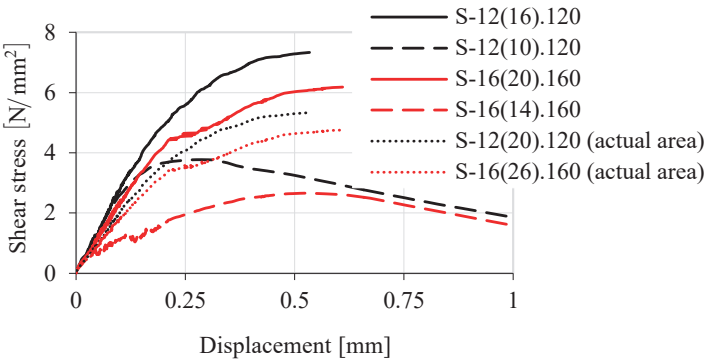

Fig. 5. The experimental shear stress-displacement curves for various specimens

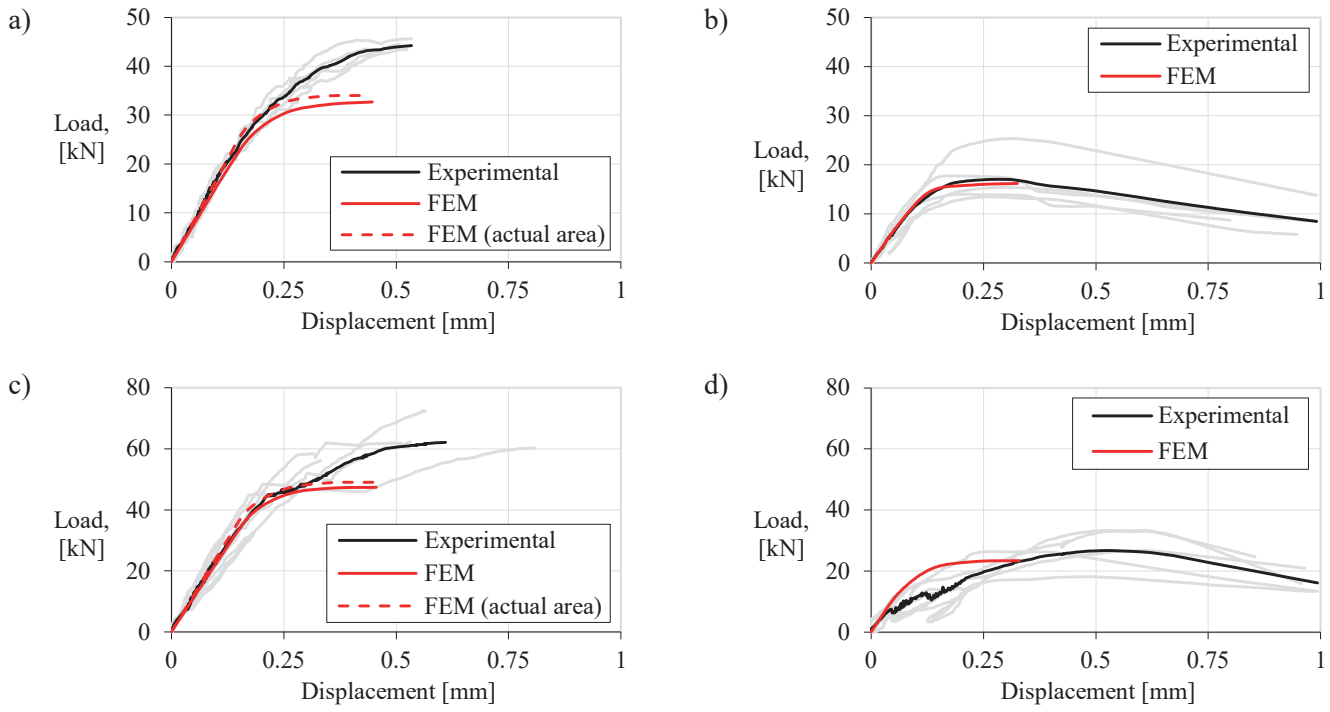

Fig. 6. Load-displacement curves of the experimental and finite element simulation: a) S-12(16).120, b) S-16(20).160, c) S-12(10).120, d) S-16(14).160

the area of the split-off timber is not even. There are some areas with no timber on the thread of the rod, as shown in Fig. 4b. Figure 5 shows that the specimens with a smaller rod diameter have higher shear stresses at the moment of failure. The stress-deformation curves of the specimens with the steel rods glued in the smaller diameter grooves show the post-failure behaviour when the contact between the steel rod and the glulam is ensured by friction.

There is no obvious maximum load point value in these graphs as the failure mode of this gluing method is ductile. The actual shear stresses are smaller than the theoretically determined ones for the specimens with the 2-mm-thick glue-line because the actual split-off timber block is bigger than the theoretical one. To theoretically determine the shear stresses the force value is divided by the area between the glue and the timber. The analysis of the dimensions of the split-off timber blocks (specimens 1, 4 and 5 from Fig. 4a) shows that the actual diameter is 6–8 mm larger than the initial diameter of the groove. The recalculated actual shear stresses are 1.3 times smaller. It is shown by the dotted lines with the note "actual shear area" in Fig. 5. The finite element modelling was also made assuming the actual shear area with the reduced shear strength, as presented in Table 2.

4.2. The numerical simulation results and their comparison with the experimental data. The finite element modelling was completed according to the methods provided in Section 3. The comparison between the experimental and the FE modelling data in terms of the load-relative displacement curves is shown in Fig. 6.

The failure of the connection in the finite element modelling occurs when the fracture criterion in Eq. (1) reaches the value of 1.0 on the whole surface between the glue-line and the timber. The maximum force in FE is determined by the interaction of several stresses, as the shear stress in the longitudinal direction amounts to only around 40%, as shown in Fig. 7. Figure 7 shows the shear stress values at the moment of failure. The maximum shear stress at the failure moment is reached in the model without a glue-line, as there is no interlayer which

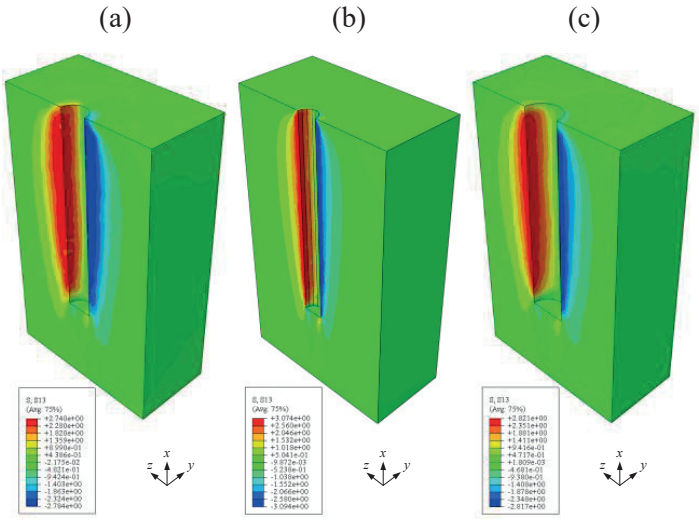

Fig. 7. The FE model of XZ-plane shear stresses (N/mm^2): a) S-12(16).120, b) S-12(10).120, c) S-12(16).120 (actual area)

redistributes stresses. As mentioned above, the experimental failure mode of the connection with the 2-mm-thick glue line is brittle, which is caused by the timber shear block's split-off. The finite element modelling is also performed evaluating the actual shear area with the reduced shear strength values. Fig. 6 shows that the models with the actual shear area and the reduced shear strength give 5–9% higher bearing capacity, and the load-displacement behavior is closer to the experimental one. The experimental bearing capacity is around 39% higher than that in the respective FE model for the specimens with the 2-mm-thick glue-line. This can be explained by the fact that the experimentally determined shear area is much larger for some specimens than that assumed in FE. Thus, the evaluation of the actual area in more detail could give the results closer to the experimental ones.

The difference of bearing capacities between two different gluing methods can mainly be explained by the shear strength value which was experimentally determined during the test. Experimental results showed that the shear strength is 1.5–1.8 times lower for the connection with groove diameter smaller than the rod's diameter. The ratio is very close to the value which was achieved during the connection finite element analysis and laboratory experiments.

The FE models without the glue-line and the experimental values are well in line, while the shear area of the experimentally extracted steel rod is even and the FE models correspond to each other.

5. Conclusions

- In this paper two different gluing methods of threaded steel rods glued in glulam are investigated: one where the connection is with the 2-mm-thick glue-line and another with a connection when the threaded steel rod is screwed into a smaller diameter groove. The steel rod is covered with glue before being screwed in.
- The two investigated different gluing methods of the threaded steel rods show different behavior at the failure moment. The connection with the 2-mm-thick glue line fails in a brittle way, while the connection with the 0-mm-thick glue-line fails in a semi ductile way and shows post-failure behavior, ensured by friction.
- To investigate the differences between these two gluing methods the connections with the same geometrical parameters were tested. The deformations between the steel rod and the glulam are practically the same, but the gluing method with the 2-mm-thick glue-line demonstrates about 2.4 times higher bearing capacity. The difference between the actual split-off timber volumes results in the differences in these two gluing methods.
- The surface-based cohesive behavior with the quadratic failure criterion was implemented to evaluate the brittle failure of the connection. The FE modelling results are well in line with the experimentally determined values. The FE modelling results show that the failure of the connection between timber and steel is determined by the interaction between several stresses, as the level of the shear stress is only around 40% at the failure moment.

References

[1] M.D.O. Chans, J.E. Cimadevila, and E. M. Gutierrez, "Model for predicting the axial strength of joints made with glued-in rods in sawn timber", *Constr. Build. Mater.* 24, 1773–1778 (2010).

[2] R. Steiger, E. Gehri, and R. Widmann, "Pull-out strength of axially loaded steel rods bonded in glulam parallel to the grain", *Mater. Struct.* 40(1), 69–78 (2007).

[3] A. Rossignon and B. Espion, "Experimental assesment of the pull-out strength of single rods bonded in glulam parallel to the grain", *Eur. J. Wood Wood Prod.* 66(6), 419–432 (2008).

[4] B.H. Xu, A. Bouchair, and P. Racher, "Analytical study and finite element modelling of timber connections with glued–in rods in bending", *Constr. Build. Mater.* 34, 337–345 (2012).

[5] N. Gattesco, A. Gubana, M. Buttazzi, and M. Moletto, "Experimental investigation on the behavior of glued-in rod joints in timber beams subjected to monotonic and cyclic loading", *Eng. Struct.* 147, 372–384 (2017).

[6] J. Ogrizovic, F. Wanninger, and A. Frangi, "Experimental and analytical analysis of moment-resisting connections with glued-in rods", *Eng. Struct.* 145, 322–332 (2017).

[7] R. Steiger, E. Serrano, M. Stepinac, et al. "Strengthening of timber structures with glued-in rods", *Constr. Build. Mater.* 97, 90–105 (2015).

[8] EN 1995-1-1:2004. Eurocode 5: design of timber structures – Part 1–1: General – common rules and rules for buildings. European Committee for Standardization.

[9] M. Verdet, J.L. Coureau, A. Cointe, and A. Salenikovich, "Creep performance of glued-in rod joints in controlled and variable climate conditions", *Int. J. Adhes. Adhes.* 75, 47–56 (2017).

[10] J. Lartigau, J.L. Coureau, S. Morel, P. Galimard, and E. Maurin, "Effect of temperature on the mechanical performnce of glued-in rods in timber", *Int. J. Adhes. Adhes.* 57, 79–84 (2015).

[11] V. Maria, L. D'Andria, G. Muciaccia, and A. Ianakiev, "Influence of elevated temperature on glued-in steel rods for timber elements", *Constr. Build. Mater.* 147, 457–465 (2017).

[12] J.L. Jensen, M. Nakatani, P. Quenneville, and B. Walford, "A simplified model for withdrawal of svrews from end-grain of timber", *Constr. Build. Mater.* 29, 557–563 (2012).

[13] M. Cepelka and K.A. Malo, "Moment rsisting splice of timber beams using long threaded rods and grout-filler couplers – Experimental results and predictive models", *Constr. Build. Mater.* 155, 560–570 (2017).

[14] H. Stamatopoulos and K.A. Malo, "Withdrawal capacity of threaded rods embedded in timber elements", *Constr. Build. Mater.* 94, 387–397 (2015).

[15] EN 14080. Timber structures – Glued laminated timber and glued solid timber. European Committee for Standardization.

[16] EN 26891 Timber structures, Joints with mechanical fasteners, General principles for determination of strength and deformation characteristics. European Committee for Standardization.

[17] N.Vasiraja and P. Nagaraj, "The effect of material gradient on the static and dynamic response of layered functionally graded material plate using finite element method", *Bull. Pol. Ac.: Tech.* 67(4), 827–838 (2019).

[18] J.I. Rojas-Sola, J.B. Bouza-Rodríguez, and A. Comesaña-Campos, "Study of ancient forging devices: 3D modelling and analysis using current computer methods", *Bull. Pol. Ac.: Tech.* 67(2), 377–390 (2019).

[19] T. Gečys, A. Daniūnas, T.K. Bader, L. Wagner, and J. Eberhardsteiner, "3D finite element analysis and experimental investigations of a new type of timber beam-to-beam connection", *Eng. Struct.* 86, 134–145, (2015).

[20] T. Gečys and A. Daniūnas, "Experimental investigation of glued laminated timber beam to beam connections filled with cement based filer", in: *Procedia engineering – 11th international conference on modern building materials, structures and techniques*, *MBMST*, 57; 320–326 (2013).

[21] ABAQUS Manual. ABAQUS 6.12 Documentation. 3DS:2012 Edition.

[22] L. Nazarko and B. Melnikas,"Operationalising Responsible Research and Innovation – tools for enterprises", *Eng. Manag. Prod. Serv.* 11(3), 21–28 (2019).

[23] C. Winkowski, "Classification of forecasting methods in production engineering", *Eng. Manag. Prod. Serv.* 11(4), 23–33 (2019).

[24] A. Šapalas, G. Šaučiuvėnas, K. Rasiulis, M. Griškevičius, and T. Gečys, "Behaviour of vertical cylindrical tank with local wall imperfections", *J. Civ. Eng. Manag.* 25(3), 287–296 2019.